Polarization selection rules in exciton-based terahertz lasers

G. Slavcheva[1,2,*] and A. V. Kavokin[3,4]

[1]*Blackett Laboratory, Imperial College London, Prince Consort Road, London SW7 2AZ, United Kingdom*

[2]*Mediterranean Institute of Fundamental Physics, Via Appia Nuova 31, 00040 Rome, Italy*

[3]*Spin Optics Laboratory, St. Petersburg State University, 1, Ulianovskaya, 198504, Russia*

[4]*School of Physics and Astronomy, University of Southampton, Highfield, Southampton SO17 1BJ, United Kingdom*

(Received 29 January 2013; revised manuscript received 12 July 2013; published 28 August 2013)

Optical pumping of excited exciton states in semiconductor quantum wells is a tool for the realization of ultracompact terahertz (THz) lasers based on stimulated optical transition between excited ($2p$) and ground ($1s$) exciton states. We show that the probability of two-photon absorption by a $2p$ exciton is strongly dependent on the polarization of both photons. Variation of the threshold power for THz lasing by a factor of 5 is predicted by switching from linear to circular pumping. We calculate the polarization dependence of the THz emission and identify photon polarization configurations for achieving maximum THz photon generation quantum efficiency.

DOI: 10.1103/PhysRevB.88.085321 PACS number(s): 78.67.De, 71.35.−y, 78.47.−p, 79.20.Ws

I. INTRODUCTION

Excitons in nanoscale semiconductor materials exhibit low-energy excitations in the range of the exciton binding energy, analogous to interlevel excitations in atoms, yielding infrared and terahertz (THz) transitions. Thus intraexcitonic transitions between excited exciton ladder states represent a natural system for generating THz radiation and coherence.

The demand for development of new compact and efficient coherent terahertz radiation sources is currently rapidly increasing due to an ever-growing range of very diverse technological applications in the relatively-little-explored THz spectrum of radiation, including sensing and communications, spectroscopy and imaging in biology and medicine, material evaluation, security, global environmental monitoring, and ultrafast computing, among others.[1] Towards this goal, recently, a scheme for a microcavity-based polariton-triggered THz laser [THz vertical cavity surface-emitting laser (VCSEL)] was proposed by one of us,[2] whereby the $2p$ dark quantum well (QW) exciton state is pumped by two-photon absorption using a cw laser beam and subsequently decays to a $1s$ exciton-polariton state emitting THz radiation.

The inverse process of strong few-cycle terahertz pulses resonantly driving an intraexcitonic $1s \rightarrow 2p$ transition in a QW has been experimentally observed and investigated in a series of works.[3] Recently, interactions of few-cycle terahertz pulses with the induced optical polarization in a QW microcavity have revealed strong coupling of the lower and higher exciton-polariton states to the $2p$ exciton state, forming a unique three-level Λ system,[4] thus enabling stimulated Raman adiabatic passage (STIRAP) coherent control techniques. On the other hand, there has been considerable experimental interest in the intraexcitonic transitions in QWs under intense THz excitation, taking advantage of the ultrafast time-resolved THz spectroscopic methods.[5] Most recently, dynamic intraexcitonic inversion and an intraexcitonic Autler-Townes effect have been observed when the intense terahertz beam is tuned near the $1s$-$2p$ transition of the heavy-hole exciton.[6]

The possibility of achieving population inversion between $1s$ (or $2s$) and $2p$ exciton states in a QW (or quantum wire) by single-photon excitation of the $1s$ or $2s$ exciton resonances has been predicted in a recent microscopic study based on semiconductor Bloch equations[7] fully including many-body effects, such as Coulomb and phonon scattering. It has been demonstrated that the incoherent $2p$ exciton state population, providing significant THz gain, can be generated by resonant pulsed excitation of the $1s$ or $2s$ exciton state. Coulomb scattering has been identified as a major many-body interaction which induces symmetry change, converting the radial s-type polarization into an incoherent p-type exciton population.

By contrast, within the framework of the proposed polariton-triggered THz laser scheme, we shall be interested in an optical cw pumping of the $2p$ exciton state by a two-photon absorption mechanism at the two-photon resonance. By resonantly pumping the $2p$ exciton state, coherent exciton population is generated. Therefore we believe that many-body effects such as the Coulomb-induced dephasing, leading to transient dynamics following an optical pulse excitation, resulting in population redistribution and generation of incoherent exciton populations, should not play a significant role.

There has been a considerable body of theoretical work on two-photon absorption in bulk semiconductors and QWs over the last decades. Two-photon absorption (TPA) in cubic bulk materials, without including excitonic effects, has been considered theoretically by Ivchenko[8,9] and most recently by Bhat *et al.*[10] (for a comprehensive list of references on TPA in bulk materials see references therein) in relation to optical spin orientation. As the two-photon absorption is a two-step process, different types of transitions can occur, depending on whether the intermediate state is in the same band as either the initial or final state or in a different band. In the former case the matrix element, corresponding to the intraband transition, is zero, in which case the transition is allowed-forbidden. There may be forbidden-allowed transitions when the conduction-band to valence-band dipole optical transition is forbidden (interband matrix element is zero at the Γ point) and the intraband transition is allowed or allowed-allowed transitions for which both matrix elements are nonzero at the Γ point. For noncentrosymmetric crystals the forbidden-allowed transitions coexist along with the p-state allowed-allowed transitions.[11] It should be noted that allowed-allowed

transitions in GaAs can dominate allowed-forbidden transitions in a frequency range close to the band edge.[10]

The polarization dependence of TPA by electrons in semiconductor heterostructures (superlattices and QWs without excitonic effects but with realistic band structure) has been calculated by Ivchenko and Pikus[12] within the single-particle picture and the Kane model, which includes $\mathbf{k}\cdot\mathbf{p}$ interaction between bands $c\Gamma_6$, $v\Gamma_8$, and $v\Gamma_7$, assuming only these three bands are virtual states of two-photon transition. Both linear and circular polarizations have been considered. The same formalism has been applied in Ref. 13 for calculation of the TPA polarization dependence in GaAs/AlGaAs heterostructures (without excitonic effects) for allowed-forbidden transitions, taking into account all actual bands [conduction (c), light hole (lh), heavy hole (hh)] and the envelope wave function of a finite barrier QW.

Two-photon transition rates of s and p exciton states in QWs have been calculated by Shimizu;[14] however, the excitons have been taken as purely two-dimensional (2D), and the sum over intermediate states has been avoided by assuming constant-energy denominators. Shimizu has found significant transition rates for transitions to s excitons for TM polarization of both pumping photons with polarization vectors $\hat{\varepsilon}_1 = \hat{\varepsilon}_2 || \hat{\mathbf{z}}$ and negligible transition rates for p excitons in the case of x polarization of both photons in the QW plane for TE polarization ($\hat{\varepsilon}_1 = \hat{\varepsilon}_2 \perp \hat{\mathbf{z}}$). Pasquarello and Quattropani[15] calculate the two-photon transition rates of discrete excitonic states beyond the simplified model by Shimizu,[14] describing the three-dimensional (3D) character of the exciton states and the QW confinement by infinite barriers. Their findings confirm Shimizu's results. In particular for p excitons, allowed for x polarization, rather small transition rates are found. Two-photon absorption reflects the dimensionality of the excitons or the squeezing of the relative motion wave function in confined geometries. A unified theory of TPA in arbitrary dimensionality has been developed by Ogawa.[16]

Despite the large number of calculations available in the literature, the polarization dependence of TPA on p excitons in QWs has been calculated only for specific polarization directions of the pumping photons. All possible polarization configurations (linear, circular, and elliptical) of the two pumping photons have not been systematically studied, and as a result the polarization selection rules in a bosonic THz laser, exploiting the THz $2p$-$1s$ transition, remain largely unknown. During the preparation of this paper, we became aware of a work[17] discussing TPA of p excitons in QWs. However, the result is only an estimate of the magnitude of the matrix element, as the quantum confinement within the QW has not been taken into account, and the polarization dependence has not been calculated.

In this paper we theoretically demonstrate polarization control of THz emission and of the quantum efficiency for THz photon generation. We consider a THz VCSEL proposed in Ref. 2, where the pump beam is split in two. Each of the split beams goes through a polarizer, so that the two photons pumping the $2p$ exciton do not necessarily have the same polarization. We show that by rotating one of the polarizers one can switch the THz laser on and off.

Using crystal-symmetry point-group theoretical methods,[12] we calculate the polarization dependence of the optical transition matrix element for two-photon excitonic absorption in GaAs/AlGaAs quantum wells, as well as of the intraexcitonic $2p$ to $1s$ THz transition radiative decay rate. This enables us to calculate the polarization dependence of the quantum efficiency for THz photon generation and thus identify maximum efficiency regimes of operation.

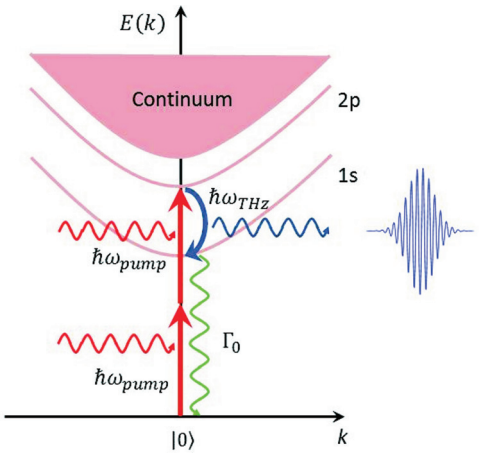

FIG. 1. (Color online) Schematic energy-level diagram of two-photon transitions to $2p$ exciton states in a QW. The ground ($1s$) and excited ($2p$ dark) discrete (bound) excitonic states and the exciton (unbound) continuum states are shown. The pumping frequency ω_{pump} is half that of the $2p$ exciton state. ω_{THz} is the center frequency of the emitted THz pulse; Γ_0 is the ground ($1s$) state exciton spontaneous emission rate.

II. TWO-PHOTON p EXCITON ABSORPTION

The optical pumping scheme of a transition to a $2p$ exciton state with two photons, each with half the energy of the $2p$ exciton state, is shown in Fig. 1.

Our first goal is to calculate the magnitude and polarization dependence of the TPA probability to p exciton states in a QW. For narrow QWs with thickness $L_z \ll 2a_B^*$, where a_B^* is the 3D exciton Bohr radius, the wave function of the quasi-2D (Q2D) exciton at the Γ point can be written as[14]

$$\Psi_\lambda(\mathbf{r}_e,\mathbf{r}_h) = \frac{v_0}{\sqrt{S}} U_\lambda^{\alpha\beta}(\rho)\Phi_c^\alpha(z_e)\Phi_v^{\beta *}(z_h)u_{c\mathbf{k}}(\mathbf{r}_e)u_{v\mathbf{k}}^*(\mathbf{r}_h)e^{i\mathbf{k}_{||}\cdot\mathbf{R}_{||}}, \quad (1)$$

where v_0 is the unit-cell volume, S is the QW area, $\mathbf{R}$ is the center-of-mass (c.m.) coordinate, $\mathbf{r} = \mathbf{r}_e - \mathbf{r}_h$ is the relative motion coordinate, $\mathbf{r}(\boldsymbol{\rho},z) = (\boldsymbol{\rho}_e - \boldsymbol{\rho}_h, z)$, with $\boldsymbol{\rho} = \boldsymbol{\rho}_e - \boldsymbol{\rho}_h$, is the in-plane relative motion coordinate, and the z axis is taken normal to the QW layers. α,β are subband indices, and $\Phi_{c(v)}^\alpha$ is the α-subband envelope function of the conduction (valence) band. $U_\lambda^{\alpha\beta}(\mathbf{r}_e - \mathbf{r}_h)$ is the envelope function of the 2D exciton associated with subbands α of the electron and β of the hole; $\lambda = (n,m)$ is the 2D exciton quantum number, labeling the discrete excitonic states ($n = 1,2,\ldots$, $|m| < n$), and $u_{c\mathbf{k}}, u_{v\mathbf{k}}$ are the periodic parts of the Bloch wave function for conduction and valence bands, respectively. The exciton c.m. wave vector $\mathbf{k}_{||}$ is on the order of the photon wave vector and therefore can be neglected and set equal to zero, thus eliminating the wave-function dependence on the c.m. motion.

Consider the case of allowed-allowed[10,12] conduction-to-valence-band dipole optical transition at the Γ point. In cubic crystals the conservation of parity upon absorption of two photons requires the final excitonic state to have the same parity as the valence band; therefore the final exciton is in a p state. The two-photon absorption probability is given by second-order perturbation theory:

$$W_{\mathrm{TPA}} = \frac{2\pi}{\hbar}\sum_{if}|V_{if}|^2 S_f(E), \tag{2}$$

where S_f is the final density of states and the momentum, $\mathbf{p}$, matrix element, V_{if}, between the initial and final states is given by[11]

$$V_{fi} = \frac{e^2}{m^2c^2}A_1A_2\sum_l\left[\frac{\langle f|\boldsymbol{\varepsilon}_1\cdot\mathbf{p}|l\rangle\langle l|\boldsymbol{\varepsilon}_2\cdot\mathbf{p}|i\rangle}{E_l - E_i - \hbar\omega_2} + \frac{\langle f|\boldsymbol{\varepsilon}_2\cdot\mathbf{p}|l\rangle\langle l|\boldsymbol{\varepsilon}_1\cdot\mathbf{p}|i\rangle}{E_l - E_i - \hbar\omega_1}\right], \tag{3}$$

reflecting the order of absorption of the first photon with polarization vector $\boldsymbol{\varepsilon}_1$, energy $\hbar\omega_1$, and vector potential A_1 and the second photon with polarization vector $\boldsymbol{\varepsilon}_2$, energy $\hbar\omega_2$, and vector potential A_2.

The excitation geometry showing the polarization vectors of the two pumping photons is depicted in Fig. 2.

Since the TPA is a two-step process, one should sum over all intermediate states $|l\rangle$ with energy E_l. Two types of matrix elements enter Eq. (3). The first is the transition matrix element from the crystal ground state that has no excitons to the intermediate states that are exciton states. This matrix element has been calculated by Elliott[18] for the 3D case and for the quasi-2D case here considered reads

$$\langle l|\hat{\varepsilon}_\mu\cdot\mathbf{p}|i\rangle = \sqrt{S}\Psi^*_\lambda(0)\langle c|\hat{\varepsilon}\cdot\mathbf{p}|v\rangle, \tag{4}$$

where $\hat{\varepsilon}_\mu$ is the first photon polarization vector with energy $\hbar\omega_1$, which may be absorbed first or second ($\mu = 1,2$), $\Psi_\lambda(0)$ is the relative motion exciton wave function evaluated at $\mathbf{r} = \mathbf{0}$, with $|\Psi_\lambda(0)|^2$ being the probability of finding the electron and the hole at the same position, and the interband matrix

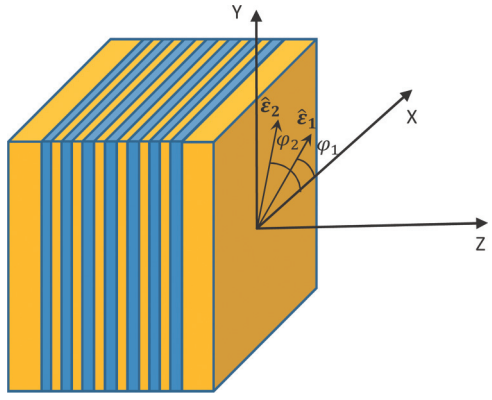

FIG. 2. (Color online) Scheme of the QW excitation geometry. The two pumping photons are generally elliptically polarized with polarization vectors $\hat{\varepsilon}_1$,$\hat{\varepsilon}_2$ lying in the QW plane, with polar angles φ_1,φ_2. The x axis of the coordinate system is fixed by a THz cavity which filters out the linear polarization of the emitted THz radiation (see Fig. 5).

element $\langle c|\hat{\varepsilon}_\mu\cdot\mathbf{p}|v\rangle$ is evaluated between the Bloch functions of conduction and valence bands:

$$\langle c|\mathbf{p}|v\rangle = \frac{1}{v_0}\int_{\mathrm{cell}} d^3r u^*_c(\mathbf{r})\frac{\hbar}{i}\nabla u_{v\hat{\mathbf{z}}}(\mathbf{r}). \tag{5}$$

Substituting the exciton wave function from Eq. (1), we obtain

$$\langle l|\hat{\varepsilon}_\mu\cdot\mathbf{p}|i\rangle = v_0U^{\alpha\beta}_\lambda(0)\Phi^\alpha_c(z_e)\Phi^{\beta*}_v(z_h)\langle c|\mathbf{p}|v\rangle. \tag{6}$$

The second matrix element entering Eq. (3) is between hydrogenic-type exciton states and can be written as

$$\begin{aligned}\frac{1}{m}\langle f|\hat{\varepsilon}_\nu\cdot\mathbf{p}|l\rangle &= \frac{1}{\bar{\mu}_\xi}\int d^3r\,\Psi^{\alpha\beta*}_\delta(\mathbf{r})(\hat{\boldsymbol{\varepsilon}}_\nu\cdot\mathbf{p})\Psi^{\alpha\beta}_\lambda(\mathbf{r})\\ &= \frac{1}{\bar{\mu}_\xi}\int d^3r\,U^{\alpha\beta*}_\delta(\rho)\Phi^{\alpha*}_c(z_e)\Phi^\beta_v(z_h)(\hat{\boldsymbol{\varepsilon}}_\nu\cdot\mathbf{p})\\ &\quad\times U^{\alpha\beta}_\lambda(\rho)\Phi^\alpha_c(z_e)\Phi^{\beta*}_v(z_h),\end{aligned} \tag{7}$$

where $\hat{\boldsymbol{\varepsilon}}_\nu$ is the second photon polarization vector with energy $\hbar\omega_2$, which may be absorbed first or second ($\nu = 1,2$), m is the free electron mass, and $\bar{\mu}_\xi$ is the reduced exciton mass along the ξ direction in the QW plane. In the above equation we have assumed that the unit-cell Bloch amplitudes are identical for the valence and conduction bands and are spherically symmetric, so that the normalization condition can be used.

Introducing special notation for the matrix element, summed over the intermediate states, according to

$$\begin{aligned}I_\delta(\mu,\nu) &= \int d^3r\,U^{\alpha\beta*}_\delta(\rho)\Phi^{\alpha*}_c(z_e)\Phi^\beta_v(z_h)(\hat{\varepsilon}_\nu\cdot\mathbf{p})\\ &\quad\times\sum_\lambda\frac{U^{\alpha\beta}_\lambda(\rho)U^{\alpha\beta*}_\lambda(0)}{E_\lambda + E_G - \hbar\omega_\mu}\\ &\quad\times\Phi^{\alpha*}_c(z_e)\Phi^\beta_v(z_h)\Phi^\alpha_c(z_e)\Phi^{\beta*}_v(z_h),\end{aligned} \tag{8}$$

where E_G is the direct interband energy gap, the total matrix element can be written as

$$\begin{aligned}V_{fi} &= \sqrt{S}\frac{e^2}{m\bar{\mu}_\xi c^2}A_1A_2[\langle c|\hat{\varepsilon}_1\cdot\mathbf{p}|v\rangle I_\delta(1,2)\\ &\quad+\langle c|\hat{\varepsilon}_2\cdot\mathbf{p}|v\rangle I_\delta(2,1)].\end{aligned} \tag{9}$$

Let us define the 2D reduced Coulomb Green's function according to

$$G(\boldsymbol{\rho},\boldsymbol{\rho}') = \sum_\lambda\frac{U^{\alpha\beta}_\lambda(\boldsymbol{\rho})U^{\alpha\beta*}_\lambda(\boldsymbol{\rho}')}{E_\lambda - \Omega}, \tag{10}$$

where E_λ is the exciton hydrogenic energy as measured from the conduction-band edge and $\Omega = -E_G + \hbar\omega_\mu < 0$. In order to evaluate the integral, we need an explicit expression for the 2D reduced Green's function. A closed form of the reduced Green's function for an unscreened exciton in three dimensions has been derived by Hostler[19] and in N dimensions by Blinder.[20] For a heavy-hole ($\alpha = c1,\beta = hh1$) QW exciton the 2D limit is of interest, and its closed form is given by Zimmermann:[21]

$$G(\rho,0) = \frac{1}{2\pi}e^{-2\rho/k_\mu a^*_B}\left[-\ln\left(\frac{4\rho}{k_\mu a^*_B}\right) - \gamma + 3 - 4\left(\frac{\rho}{k_\mu a^*_B}\right)\right], \tag{11}$$

where a_B^* is the 3D exciton Bohr radius, γ is Euler's constant, and

$$k_\mu^2 = \frac{E_B}{E_G - \hbar\omega_\mu}, \tag{12}$$

with $E_B \equiv \mathrm{Ry}^*$ being the exciton binding energy. Introducing cylindrical coordinates, the polarization dependence in Eq. (8) can be written as

$$\hat{\varepsilon}_\nu \cdot \mathbf{p}G(r,0) = -i\hbar(\hat{\boldsymbol{\varepsilon}}_\nu \cdot \hat{\boldsymbol{\rho}})\frac{\partial}{\partial\rho}G(\rho,0)\Phi_c^\alpha(z_e)\Phi_v^{\beta*}(z_h) - i\hbar(\hat{\boldsymbol{\varepsilon}}_\nu \cdot \hat{\mathbf{z}})G(\rho,0)\frac{\partial}{\partial z}\left[\Phi_c^\alpha(z)\Phi_v^{\beta*}(z)\right],$$

where $\hat{\boldsymbol{\rho}} = \frac{\boldsymbol{\rho}}{|\boldsymbol{\rho}|}$ and $\hat{\mathbf{z}}$ are unit vectors. Introducing the overlap integral of the subband envelope wave functions,

$$I_{\alpha\beta} = \left\langle \Phi_c^\alpha(z)\middle|\Phi_v^\beta(z)\right\rangle = \int dz\, \Phi_c^{\alpha*}(z)\Phi_v^\beta(z), \tag{13}$$

and momentum matrix element along the z direction,

$$P_{\alpha\beta} = \left\langle \Phi_c^\alpha(z)\middle|p_z\middle|\Phi_v^\beta(z)\right\rangle = \int dz\, \Phi_c^{\alpha*}(z)\frac{\hbar}{i}\frac{\partial}{\partial z}\Phi_v^\beta(z), \tag{14}$$

Eq. (8) can be recast as

$$I_\delta(\mu,\nu) = -i\hbar\frac{v_0^2}{S}\left[I_{\alpha\beta}\int d^2\rho U_\delta^{\alpha\beta*}(\rho)(\hat{\boldsymbol{\varepsilon}}_\nu \cdot \hat{\boldsymbol{\rho}})\frac{\partial G(\rho,0)}{\partial\rho} + P_{\alpha\beta}\int d^2\rho U_\delta^{\alpha\beta*}(\rho)(\hat{\boldsymbol{\varepsilon}}_\nu \cdot \hat{\mathbf{z}})G(\rho,0)\right]. \tag{15}$$

For the VCSEL configuration we shall be interested in the normal incidence geometry; i.e., we choose $\hat{\varepsilon}_\nu \perp z$, and therefore the second term in Eq. (15) vanishes. The integration in the QW plane is performed in polar coordinates (ρ,φ):

$$I_\delta(\mu,\nu) = -i\pi\hbar I_{\alpha\beta}\int_0^\infty d\rho\, \rho\, U_\delta^{\alpha\beta*}(\rho)\frac{\partial G(\rho,0)}{\partial\rho}. \tag{16}$$

The problem is reduced therefore to the evaluation of the integral over the ρ coordinate in the QW plane, given in Appendix A. As the two photons may be absorbed in either order (1, 2 and 2, 1), substituting in Eq. (9), we obtain the following expression for the excitonic two-photon absorption matrix element:

$$V_{fi} = \frac{v_0^2}{\sqrt{S}}\frac{e^2}{mc^2}A_1A_2\frac{4\hbar I_{\alpha\beta}}{3\pi i\sqrt{3\pi}}\frac{1}{E_B a_B^{*2}}J_{\mathrm{eff},2}\langle c|\mathbf{p}|v\rangle, \tag{17}$$

where we have defined the effective matrix element for cubic crystals, using the invariance of the interband matrix element $M = \langle c|\mathbf{p}|v\rangle$ under crystal point-symmetry-group transformations,[11,12,22,23] whereby the interaction term is split into antisymmetric and symmetric parts according to

$$\begin{aligned} J_{\mathrm{eff},2}^2 &= \frac{1}{2}(\hat{\boldsymbol{\varepsilon}}_1 \times \hat{\boldsymbol{\varepsilon}}_2)^2|J_{p,2}(k_1) - J_{p,2}(k_2)|^2 \\ &\quad + \frac{1}{2}[1 + (\hat{\boldsymbol{\varepsilon}}_1 \cdot \hat{\boldsymbol{\varepsilon}}_2)^2]|J_{p,2}(k_1) + J_{p,2}(k_2)|^2 \\ &= \frac{C_1^2}{2}\left\{(\hat{\boldsymbol{\varepsilon}}_1 \times \hat{\boldsymbol{\varepsilon}}_2)^2\left|k_1^2 - k_2^2\right|^2 \right. \\ &\quad \left. + [1 + (\hat{\boldsymbol{\varepsilon}}_1 \cdot \hat{\boldsymbol{\varepsilon}}_2)^2]\left|k_1^2 + k_2^2\right|^2\right\}. \end{aligned} \tag{18}$$

Substituting Eqs. (A4)–(A6) back in Eq. (2), we finally get for the excitonic two-photon absorption probability to $2p$ exciton states (in $\mathrm{s}^{-1}\,\mathrm{m}^{-2}$)

$$W_{2p}^{(2)} = K_{\mathrm{TPA}}\frac{1}{27\pi^3}I_{\alpha\beta}^2M^2\left(\frac{\hbar^2}{a_B^{*4}}\right)J_{\mathrm{eff},2}^2S_{2p}^{c1,hh1}, \tag{19}$$

where $S_{2p}^{c1,hh1}$ is the final $2p$ exciton density of states per unit surface for a heavy-hole exciton (c1-hh1).

For an infinite QW with well width L_z the envelope wave functions are of the form (see, e.g., Ref. 24)

$$\Phi_{c(v)}^{c1\,(hh1)}(z) = \sqrt{\frac{2}{L_z}}\cos\left[(2p+1)\frac{\pi z}{L_z}\right], \quad p = 0,1,2,3,\ldots \tag{20}$$

The coefficient K_{TPA} is calculated taking into account the normalization of the above subband envelope functions, yielding

$$K_{\mathrm{TPA}} = \frac{128\pi e^4A_1^2A_2^2v_0^2}{\hbar\bar{\mu}_\xi^2m^2c^4SL_z^2E_B^2}. \tag{21}$$

Our pumping scheme envisages two photons, each with half the energy of the $2p$-exciton state, $\hbar\omega_1 = \hbar\omega_2 = \hbar\omega = \frac{E_{2p}}{2}$ and $k_1^2 = k_2^2 = k^2 = \frac{2E_B}{2E_G - E_{2p}}$; therefore the first term in Eq. (18) vanishes, yielding

$$W_{2p}^{(2)} = \frac{K_{\mathrm{TPA}}}{27\pi^3}\frac{C_1^2}{2}M^2I_{\alpha\beta}^2\left(\frac{\hbar^2}{a_B^{*4}}\right)S_{2p}^{c1,hh1} \times \frac{16E_B^2}{(2E_G - E_{2p})^2}[1 + (\hat{\boldsymbol{\varepsilon}}_1 \cdot \hat{\boldsymbol{\varepsilon}}_2)^2]. \tag{22}$$

The polarization dependence of the exciton two-photon transition probability in the above equation is given by

$$\begin{aligned} P(\hat{\boldsymbol{\varepsilon}}_1,\hat{\boldsymbol{\varepsilon}}_2) &= 1 + (\hat{\boldsymbol{\varepsilon}}_1 \cdot \hat{\boldsymbol{\varepsilon}}_2)^2 \\ &= 1 + [\cos\varphi_1\cos\varphi_2 + \cos(\varphi_1 + \delta_1)\cos(\varphi_2 + \delta_2)]^2, \end{aligned}$$

where the photon polarization vectors $\hat{\boldsymbol{\varepsilon}}_1,\hat{\boldsymbol{\varepsilon}}_2$ lie in the QW plane subtending polar angles φ_1,φ_2 to the x axis, fixed by the linear polarization direction filtered out of the THz cavity, and phase shifts δ_1,δ_2, respectively (see Fig. 2).

Depending on the phase shift of the first/second photon, one gets generally elliptically polarized photons, which for the special case of $\delta_1,\delta_2 = m\pi$, $m = 0,\pm1,\pm2,\ldots$ degenerates to linear and for

$$\delta_1,\delta_2 = \begin{cases} \frac{\pi}{2} + 2m\pi, & \sigma^+ \\ -\frac{\pi}{2} + 2m\pi, & \sigma^- \end{cases}, \quad m = 0,\pm1,\pm2,\ldots$$

degenerates to right- or left-circular polarization.

Three-dimensional and contour plots of the polarization dependence of the exciton two-photon absorption probability are shown in Fig. 3 for different polarizations of the two pumping photons.

We suggest adding an external THz cavity at the VCSEL output, which will filter out the linear polarization of the emitted THz radiation and will thus constitute our reference frame, fixing the direction of the coordinate system x axis. We shall assume that the generated THz mode is X polarized. By inspection of Fig. 2 one can see that the maximum (fivefold) increase of the two-photon absorption rate with respect to

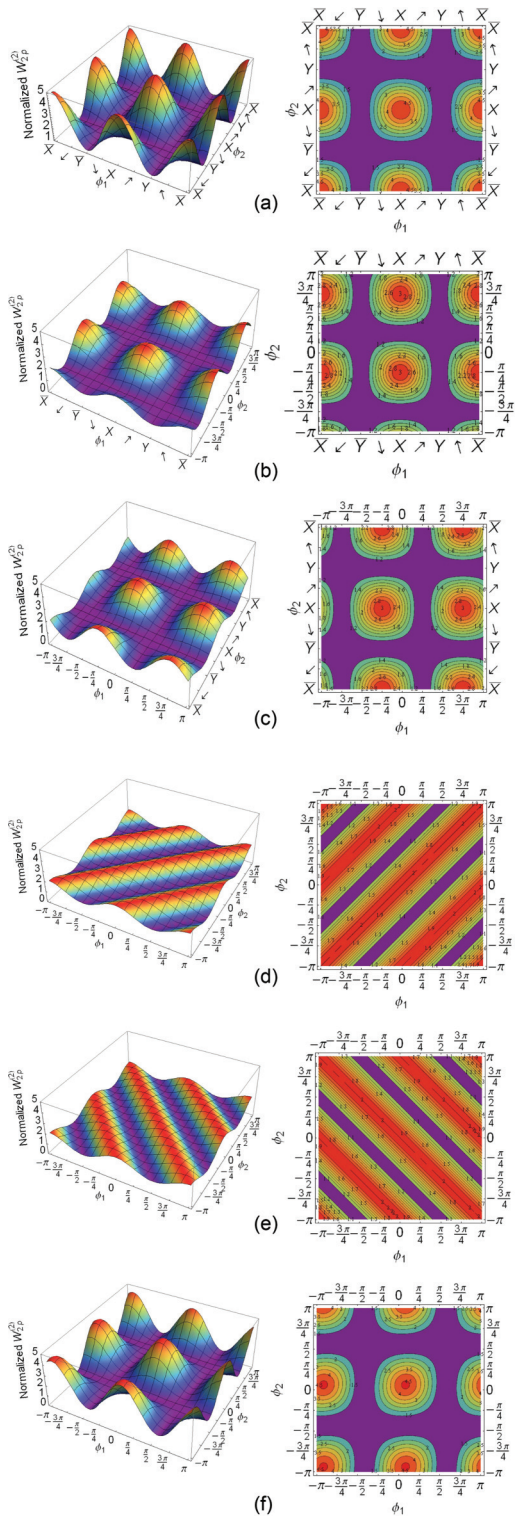

FIG. 3. (Color online) Three-dimensional surface and contour plots of the normalized excitonic two-photon absorption against polar angles of $\hat{\varepsilon}_1$ and $\hat{\varepsilon}_2$ in the QW plane at specific phase shifts δ_1,δ_2. (a) Colinearly polarized photons $\delta_1 = 0, \pm\pi$, $\delta_2 = 0, \pm\pi$. (b) First linear and second σ^+ circularly polarized photons $\delta_1 = 0$, $\delta_2 = \frac{\pi}{2}$. (c) First σ^+ circularly polarized photon and second linearly polarized photon $\delta_1 = \frac{\pi}{2}$, $\delta_2 = 0$. (d) σ^+-σ^+ or σ^--σ^- cocircularly polarized photons $\delta_1 = \pm\frac{\pi}{2}$, $\delta_2 = \pm\frac{\pi}{2}$. (e) σ^+-σ^- or σ^--σ^+ countercircularly polarized photons $\delta_1 = \pm\frac{\pi}{2}$, $\delta_2 = \mp\frac{\pi}{2}$. (f) Co-left-elliptically polarized photons $\delta_1 = -\frac{\pi}{6}$, $\delta_2 = -\frac{\pi}{8}$.

YY polarization is achieved for linearly $XX, X\bar{X}, \bar{X}X, \bar{X}\bar{X}$ polarized photons [Fig. 3(a)]. The two-photon absorption rate can increase by a factor of 3 for linearly-circularly or circularly-linearly polarized photons [Figs. 3(b) and 3(c)], by a factor of 2 for both circularly polarized photons [Figs. 3(d) and 3(e)], and by a factor close to 5 (but always less than the one for linear polarization) for elliptically polarized photons [Fig. 3(f)]. Our results show that changing polarization from YY to XX, passing through circularly and elliptically polarized pumping, one can vary the lasing threshold by a factor of 5. The fivefold increase of the exciton TPA probability for linear polarization along the p state, compared to the one in the orthogonal direction, is an unexpected result, which we consider a direct consequence of the crystal point-group symmetry at the Γ point for direct allowed-allowed transitions in cubic semiconductors.

III. INTRAEXCITONIC $2p \rightarrow 1s$ TRANSITION PROBABILITY

To estimate the quantum efficiency of THz photon generation, we need to calculate the polarization dependence of the $2p \rightarrow 1s$ photon intraexcitonic transition, generating THz emission (Fig. 1). We are interested in the optical transition matrix element between the initial twofold-degenerate state Ψ_δ with $\delta = (n = 2, m = \pm 1) = (2, p)$ and the final state Ψ_λ with $\lambda = (n = 1, m = 0) = (1, s)$. The matrix element is of the second type in the two-photon absorption rate calculation above, Eq. (7), and is given by

$$M_{lf} = \langle f|\hat{\boldsymbol{\varepsilon}}\cdot\mathbf{p}|l\rangle = \frac{m}{\bar{\mu}_\xi}\int d^3r_e \int d^3r_h \Psi_\delta^{\alpha\beta *}(\mathbf{r}_e,\mathbf{r}_h)(\hat{\boldsymbol{\varepsilon}}\cdot\mathbf{p})\Psi_\lambda^{\alpha\beta}(\mathbf{r}_e,\mathbf{r}_h), \tag{23}$$

where the exciton wave function is given by Eq. (1). The integration over the hole coordinates is performed with $\delta(\rho_e - \rho_h)$ and $\delta(z_e - z_h)$. Choosing $\hat{\varepsilon}\perp\hat{z}$, the intraexcitonic matrix element can be written as

$$M_{lf} = \frac{v_0^2}{S}\left(\frac{m}{\bar{\mu}_\xi}\right) I_{\alpha\beta}^2 \int d^2\rho\, U_\delta^{\alpha\beta *}(\rho)(\hat{\boldsymbol{\varepsilon}}\cdot\hat{\boldsymbol{\rho}})\frac{\partial}{\partial\rho}U_\lambda^{\alpha\beta}(\rho). \tag{24}$$

In deriving Eq. (24) we have used the normalization of the Bloch amplitudes, which are assumed to be identical for the conduction and valence bands and also to be spherically symmetric.

Consider transitions from $1s$ to p-like exciton states with quantum number n. The intraexcitonic matrix element is evaluated in Appendix B using 2D hydrogen atom approximation for the relative-motion exciton wave function. We find that the angular dependence is given by $\Phi(\varphi) = \cos\varphi\, e^{\mp i\varphi}$.

Substituting the above calculated matrix element back into Fermi's golden rule, Eq. (2), the $2p \rightarrow 1s$ intraexcitonic optical transition probability is obtained as

$$W^{(2)}_{2p\rightarrow 1s} = \frac{2\pi}{\hbar}\left(\frac{e}{\bar{\mu}c}\right)^2 (A_{\mathrm{THz}})^2 \frac{\hbar^2 v_0^2}{S}\frac{27}{512}\frac{1}{\pi^2 a_B^{*2}} I_{\alpha\beta}^4 S_{1s}(E)\Phi^2(\varphi), \tag{25}$$

where $S_{1s}(E)$ is the final ($1s$) state density of states (line-shape function) and $A_{\rm THz}$ is the THz photon vector potential.

The amplitude of the THz vector potential can be expressed in terms of the THz emission intensity $I_{\rm THz}$. This can be done by equalizing the time average of the energy density of an electromagnetic wave in a medium with refractive index n to the energy density of photons (see, e.g., Ref. 27),

$$\frac{1}{2\pi}n^2\left(\frac{\omega}{c}\right)^2 A^2 = N\hbar\omega, \tag{26}$$

where N is the number of photons per unit volume, and introducing THz photon intensity according to

$$I_{\rm THz} = N\hbar\omega\,\frac{c}{n}. \tag{27}$$

Finally, the following expression is obtained (cf. Ref. 12):

$$A_{\rm THz} = \left(\frac{2\pi c I_{\rm THz}}{n\omega_{\rm THz}^2}\right)^{1/2}, \tag{28}$$

where $\omega_{\rm THz} = \frac{E_{2p}-E_{1s}}{\hbar}$.

Using the normalization condition for the infinite quantum well envelope functions [see Eq. (20)], we obtain

$$W^{(2)}_{2p\to 1s} = \frac{27}{512}K^{\rm THz}_{\rm OPA}\frac{\hbar^2}{\pi^2 a_B^{*2}}I^4_{\alpha\beta}S_{1s}(E)\Phi^2(\varphi), \tag{29}$$

where the one-photon THz emission coefficient is given by

$$K^{\rm THz}_{\rm OPA} = \frac{16\pi}{\hbar}\left(\frac{e}{\bar{\mu}_\xi c}\right)^2\frac{v_0^2 A^2_{\rm THz}}{L_z^4 S}. \tag{30}$$

The polarization dependence of the THz emission rate can be inferred from the angular dependence: for linear (e.g., along the x axis) polarization of the emitted THz photon ($\hat{\varepsilon}||\,\hat{\mathbf{x}}$), $\Phi^2(\varphi) = 1$, and for y-linear polarization $\hat{\varepsilon}||\,\hat{\mathbf{y}}$, $\Phi^2(\varphi) = 0$; therefore there is no THz emission, and for a circularly polarized THz photon, $\Phi^2(\varphi) = \frac{1}{2}$, the corresponding THz emission rate is half of the one for x-linear polarization.

IV. QUANTUM EFFICIENCY OF TERAHERTZ PHOTON GENERATION

We are interested in the quantum efficiency for THz photon generation by two-photon absorption pumping. The quantum efficiency of THz radiation generation can be defined as the ratio of the THz photon generation rate and the two-photon absorption rate by a $2p$ exciton. Following Ref. 2, the THz photon generation rate is given by $T = W_G N_p(N_s+1)$, where N_p is the population of a $2p$ exciton state, N_s is the population of the final $1s$ state, and $W_G = \frac{2G^2}{\hbar\zeta}$, where G is the oscillator strength of the $2p\to 1s$ radiative transition and ζ is the average inverse broadening of the states in the system. The two-photon pumping term is given by $P = \frac{1}{2}W_g g^{(2)}(0)N_a^2$, where N_a is the photon number in the pumping mode, $g^{(2)}(0)$ is the second-order coherence, and $W_g = \frac{4g^2}{\hbar\zeta}$, where g is the oscillator strength of the two-photon absorption. The quantum efficiency can then be expressed as

$$\eta = \frac{T}{P} = \left(\frac{G}{g}\right)^2\frac{N_p(N_s+1)}{g^{(2)}(0)N_a^2}. \tag{31}$$

Therefore the quantum efficiency of THz photon generation depends on the ratio r of the oscillator strengths of the respective transitions:

$$r = \left(\frac{G}{g}\right)^2. \tag{32}$$

The above ratio can be expressed in terms of the transition probabilities of the respective transitions (see Appendix C) as

$$r = \frac{\omega_{2p}^2}{\omega_{\rm THz}^2}\frac{W^{(2)}_{2p\to 1s}}{W^{(2)}_{2p}}. \tag{33}$$

Substituting the expressions for the transition probabilities of the $2p\to 1s$ transition from Eq. (29) and the two-photon transition to $2p$ exciton states from Eq. (19), after some algebra one can obtain

$$\eta = \frac{144m^2n^2a_B^{*2}SI^2_{\alpha\beta}}{e^2\hbar^2L_zM^2\left[143+36\ln\left(\frac{2}{3}\right)\right]^2}\frac{E^4_{2p}(2E_G-E_{2p})^2}{(E_{2p}-E_{1s})^3} \times\left(\frac{S^{c1,hh1}_{1s}}{S^{c1,hh1}_{2p}}\right)P(\hat{\boldsymbol{\varepsilon}}_1,\hat{\boldsymbol{\varepsilon}}_2,\hat{\boldsymbol{\varepsilon}}), \tag{34}$$

where we have used Eq. (28) and an expression for the pump intensity $I_{\rm pump}$ in terms of the power in the pumping laser beam:

$$I_{\rm pump} = N_a\hbar\omega_{\rm pump}\frac{c}{Vn} = \frac{N_a}{V}\frac{E_{2p}}{2}\frac{c}{n}, \tag{35}$$

where $V = SL_z$ is the QW volume, $n_a = N_a/V$ is the number density of photons per unit volume in the pumping mode, and we are pumping with photons that have half the energy of the $2p$ exciton state, i.e., $\hbar\omega_{\rm pump} = \frac{E_{2p}}{2}$. A similar expression for the THz radiation intensity $I_{\rm THz}$ can be obtained:

$$I_{\rm THz} = N_c\hbar\omega_{\rm THz}\frac{c}{Vn} = \frac{N_c}{V}(E_{2p}-E_{1s})\frac{c}{n}, \tag{36}$$

where N_c is the occupation photon number in the THz radiation mode.

The interband matrix element in Eq. (34), depending on the polarization, is given by $M_x = \langle c|p_x|v\rangle$, $M_y = \langle c|p_y|v\rangle$ for linear polarization and $M_{\rm circ} = \langle c|\frac{1}{\sqrt{2}}(p_x \pm ip_y)|v\rangle$ for circular polarization.

The polarization dependence of the quantum efficiency is given by

$$\begin{aligned} &P(\hat{\varepsilon}_1,\hat{\varepsilon}_2,\hat{\varepsilon}) \\ &\quad= \frac{\Phi^2(\varphi)}{1+(\hat{\boldsymbol{\varepsilon}}_1\cdot\hat{\boldsymbol{\varepsilon}}_2)^2} \\ &\quad= \frac{\cos^2(\varphi)}{1+[\cos\varphi_1\cos\varphi_2+\cos(\varphi_1+\delta_1)\cos(\varphi_2+\delta_2)]^2}, \end{aligned} \tag{37}$$

where φ is the polar angle of the THz photon polarization in the QW plane.

Assuming that the $2p$ exciton excited by two-photon absorption has a lifetime long enough that it loses any memory of the polarization and phase of the excitation and can emit with any polarization, we consider emission with one polarization (linear or circular) and all possible choices of polarization of the two pumping photons.

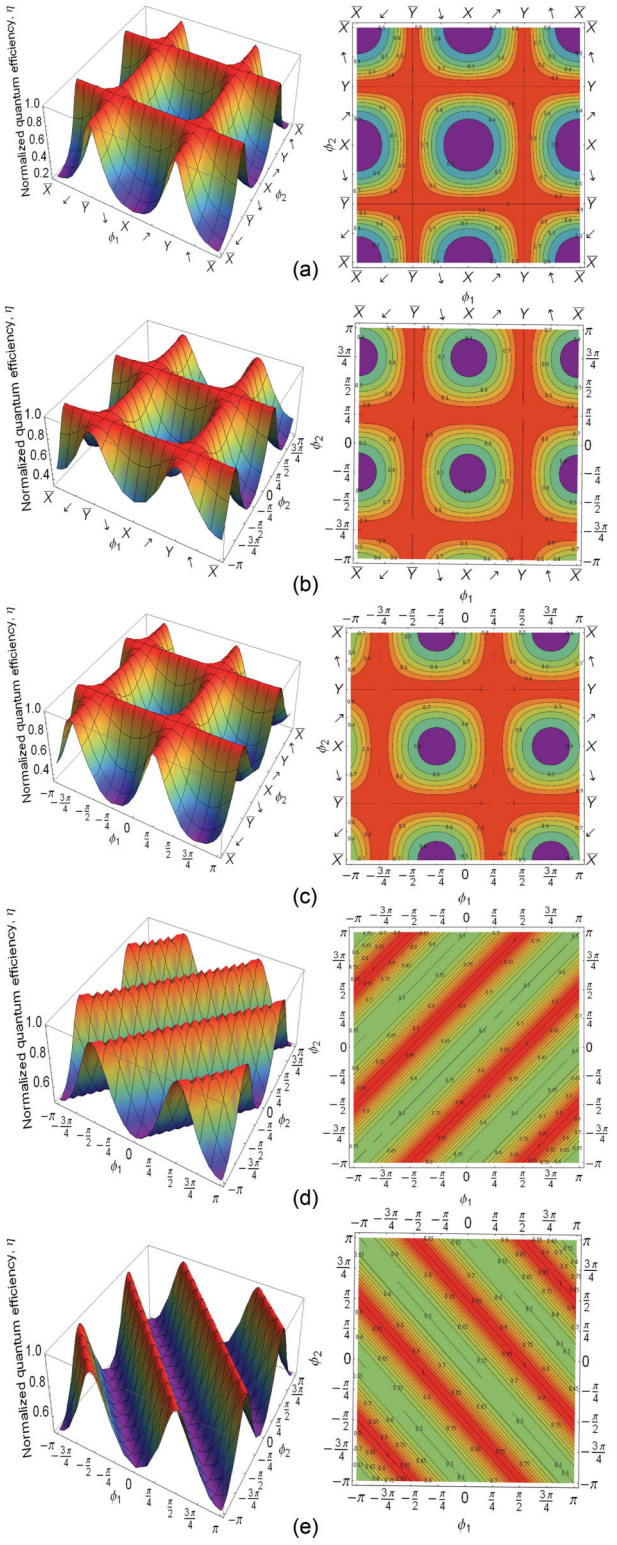

FIG. 4. (Color online) Three-dimensional surface (left) and contour (right) plots of the normalized quantum efficiency of THz photon generation against polar angles of the pumping photon polarization vectors in the QW plane at different phase shifts δ_1,δ_2 at linear $\phi = 0, \pm\pi$ polarization of the emitted THz radiation. (a) Colinearly polarized photons. (b) First linear and second circularly polarized photons. (c) First circular and second linearly polarized photons. (d) σ^+-σ^+ or σ^--σ^- cocircularly polarized photons. (e) σ^+-σ^- or σ^--σ^+ countercircularly polarized photons.

The quantum efficiency polarization dependence is shown in Fig. 4 for different polarization configurations of the two pumping photons at a given (linear) emitted THz photon polarization. Maximum quantum efficiency $\eta = 1$ is achieved along YY lines for colinearly polarized photons, for the Y-polarized first (second) photon in the case of linear-circular (circular-linear) polarization, or along diagonal lines for co- and counter-circular-circular polarization of the pumping photons. The plots for circularly polarized THz radiation look exactly the same but are scaled down by a factor of 2 (not shown), resulting in maximum efficiency $\eta = 0.5$. In addition to the results presented in Fig. 4, we note that maximum quantum efficiency $\eta = 1$ for linearly polarized ($\phi = 0,\pi$) and $\eta = 0.5$ for circularly polarized ($\varphi = \frac{\pi}{4}$) THz emission is achieved for counter-$X(\bar{X})$-linearly polarized pumping photons $\delta_1 = 0(\pi),\delta_2 = \pi(0)$ for any direction of the linear polarization of the two pumping photons in the QW plane. This is an unexpected result from our group-theoretical calculations. Furthermore, if the THz emission is Y linearly polarized, the quantum efficiency $\eta = 0$; i.e., no THz radiation should be emitted in this case. We emphasize that although maximum quantum efficiency could be achieved both by counter- and colinearly polarized photons, the quantum efficiency in the former case is constant, while in the latter it is obtained solely for specific orientations in the QW plane (YY, orthogonal to the p exciton state).

In order to verify these predictions experimentally, one can envisage pumping a QW structure with two laser beams having the same frequency (equal to half of the $2p$ exciton resonance frequency) but different polarizations. These two beams may be generated by the same laser but should propagate through different polarizers before focusing on the sample (see Fig. 5). In addition, we suggest including a delay line between the two parts of the pumping beam, which would provide the phase difference of π between them to obtain counterlinearly polarized beams for which unconditional maximum efficiency is predicted. The intensity and polarization of the emitted THz light could be measured as a function of intensities and polarizations of the two pumping beams. As reference experiments one can measure the intensity of the THz emission with one of the pump beams switched off. Analyzing the results of such experiments, one should bear in mind that the two photons used to generate a $2p$ exciton may originate from the same beam or from different beams. Comparing the spectra obtained with both beams switched on with those obtained

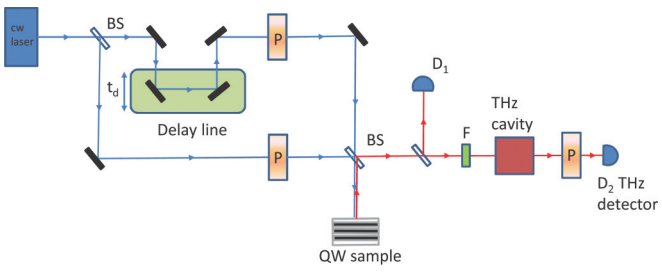

FIG. 5. (Color online) Scheme of the suggested experimental setup for polarization control of the THz VCSEL. The delay line provides the phase difference of π. BS: beam splitter, P: polarizer, F: band-pass filter, D1: visible light detector, D2: THz detector.

with only the first or second beam switched on, one can extract the signal generated by absorption of the two photons coming from different beams and thus having different polarizations.

V. CONCLUSIONS

In conclusion, we have developed a theory of the two-photon excitonic absorption to p exciton states in QWs and calculated the polarization dependence of two-photon transition probability, using crystal-symmetry point-group theory. We show that the two-photon transition rate is strongly dependent on the polarization of both pumping photons and our model predicts variation of the lasing threshold by a factor of 5 by switching pumping photons polarization from colinearly polarized along the p state to colinearly polarized in an orthogonal direction. We calculate also the polarization dependence of the intraexcitonic THz emission and the quantum efficiency for THz photon generation. Our theory predicts maximum quantum efficiency for counterlinearly polarized pumping photons and linearly polarized THz transition. Conditions for achieving maximum quantum efficiency for different polarizations of the pumping photons are identified, thereby opening routes for polarization control of the THz VCSEL and a whole new range of applications resulting from it.

We believe the two-photon resonance cw excitation scheme is inherently robust against Coulomb-induced dephasing processes, as coherent p exciton populations are generated by the two-photon resonant excitation and crystal-symmetry point-group-allowed transitions are considered, rather than transient incoherent exciton population redistribution. However, in view of assessing the viability of the proposed scheme, we envisage, as a future project, quantifying the effect of the Coulomb scattering, for instance. This can be done by extending our single-particle exciton Green's function description to fully include many-body effects, such as Coulomb screening, pair correlations, and phase-space filling, by employing a nonequilibrium Green's-function approach.

ACKNOWLEDGMENTS

We thank Professor E. L. Ivchenko for valuable discussions. A.K. acknowledges financial support from the EPSRC Established Career Fellowship grant.

APPENDIX A: INTEGRAL EVALUATION

In order to evaluate the integral in Eq. (16), we note first that the derivative of the Green's function is easily carried out using Eq. (11), giving

$$\frac{\partial G(\rho,0)}{\partial \rho} = \frac{1}{\pi k_\mu a_B^*} e^{-\frac{2\rho}{k_\mu a_B^*}} \left[\ln\left(\frac{4\rho}{k_\mu a_B^*}\right) + \gamma - 5 + \frac{4\rho}{k_\mu a_B^*} - \frac{k_\mu a_B^*}{2\rho} \right]. \tag{A1}$$

We take the exciton relative motion wave function to be the 2D hydrogen atom wave function for bound exciton states:[25,26]

$$U_{nm}^{\alpha\beta}(\boldsymbol{\rho}) = N_{nm} \left(\frac{2\rho}{a_B^*\left(n-\frac{1}{2}\right)}\right)^{|m|} e^{-\frac{\rho}{a_B^*(n-\frac{1}{2})}} \times L_{n+|m|-1}^{2|m|}\left(\frac{2\rho}{a_B^*\left(n-\frac{1}{2}\right)}\right) e^{im\phi}, \quad n = 1,2,3,\ldots,|m| < n, \tag{A2}$$

where $N_{nm} = [\frac{(n-1-|m|)}{\pi a_B^{*2}(n-\frac{1}{2})^3[(n-1+|m|)!]^3}]^{1/2}$ and $L_n^\alpha(x)$ are associated Laguerre polynomials.[28]

For the general case of a two-photon optical transition to the nth p exciton state $\delta = (n,1)$, after carrying out the angular integral and introducing dimensionless parameter k_μ, according to Eq. (12), we obtain

$$I_{n,1}(\mu,\nu) = -\frac{i\hbar N_{n1} I_{\alpha\beta}(k_\mu a_B^*)^2}{4\pi} \int_0^\infty dx\, x^2 L_n^2(x) e^{-\frac{3}{2}x} \times \left[\ln(2x) + \gamma - 5 + 2x - \frac{1}{x}\right], \tag{A3}$$

where $x = \frac{2\rho}{k_\mu a_B^*}$ and $N_{n1} = [\frac{(n-2)!}{\pi a_B^{*2}(n-\frac{1}{2})^3(n!)^3}]^{1/2}$. However, no closed form is available for the integral above.

We are interested in two-photon optical transitions to $2p$ exciton states with $n = 1, m = \pm 1$, for which we obtain

$$I_{2,1}(\mu,\nu) = \frac{4\hbar I_{\alpha\beta}}{3\pi i\sqrt{3\pi} k_\alpha a_B^{*5} E_B} J_{p,2}(k_\mu), \tag{A4}$$

where $E_B = \frac{\hbar^2}{2\bar{\mu}_\xi a_B^{*2}}$ is the exciton binding energy and the integral $J_{p,2}$ is given by

$$J_{p,2}(k_\mu) = \int_0^\infty d\rho\, \rho^2 e^{-\frac{8\rho}{3k_\alpha a_B^*}} L_2^2\left(\frac{4\rho}{3k_\mu a_B^*}\right) \times \left[\ln\left(\frac{4\rho}{k_\mu a_B^*}\right) + \gamma - 5 + \frac{4\rho}{k_\mu a_B^*} - \frac{k_\mu a_B^*}{2\rho}\right]. \tag{A5}$$

The above integral can be carried out and gives

$$J_{p,2}(k_\alpha) = -C_1 a_B^{*3} \kappa_\alpha^3, \tag{A6}$$

with $C_1 = -\frac{9[143+36\ln(\frac{2}{3})]}{2048}$.

APPENDIX B: EVALUATION OF THE INTRAEXCITONIC MATRIX ELEMENT

Let us consider transitions from $1s$ to p-like exciton states with quantum number n. We shall assume that the exciton wave function is well approximated by the 2D hydrogen atom wave function for the bound states, given by Eq. (A2). The exciton wave function for the $1s$ exciton with $n = 1, m = 0$ is then obtained:

$$U_{10}^{\alpha\beta}(\rho) = 2\left(\frac{2}{\pi a_B^{*2}}\right)^{1/2} e^{-\frac{2\rho}{a_B^*}}, \tag{B1}$$

where $\alpha = c1$, $\beta = hh1$ for the heavy-hole exciton. The 2D exciton wave function of a np exciton with quantum numbers

$n,m = \pm 1$ is given by

$$U_{n1}^{\alpha\beta}(\rho) = \left[\frac{(n-2)!}{\pi a_B^{*2}\left(n-\frac{1}{2}\right)^3 (n!)^3}\right]^{1/2} e^{-\frac{\rho}{a_B^*(n-\frac{1}{2})}} \times \left(\frac{2\rho}{a_B^*\left(n-\frac{1}{2}\right)}\right) L_n^2\left(\frac{2\rho}{a_B^*\left(n-\frac{1}{2}\right)}\right) e^{\pm i\varphi}. \quad \text{(B2)}$$

The momentum matrix element for optical transitions to $2p$ exciton states then reads

$$M_{lf} \equiv \langle \Psi_{2,\pm 1}|\mathbf{p}|\Psi_{1,0}\rangle = \frac{v_0^2}{S}\left(\frac{-8\hbar}{i}\right)\left(\frac{m}{\bar{\mu}_\xi}\right) I_{\alpha\beta}^2 \left(\frac{1}{3\sqrt{3}}\right)\frac{2\sqrt{2}}{3\pi a_B^{*4}}\Phi(\varphi) \times \int d\rho\, \rho^2 e^{-\frac{8\rho}{3a_B^*}} L_2^2\left(\frac{4\rho}{3a_B^*}\right), \quad \text{(B3)}$$

where we have introduced polar coordinates and the angular dependence is given by $\Phi(\varphi) = \cos\varphi\, e^{\mp i\varphi}$. The integration over ρ is easily performed, giving $\frac{81}{512}a_B^{*3}$.

APPENDIX C: OSCILLATOR STRENGTHS RATIO

The oscillator strength of a $|1\rangle \to |2\rangle$ transition between exciton states with energies E_1 and E_2 is a dimensionless quantity defined according to

$$f_{12} = \frac{2\bar{\mu}_\xi}{e^2\hbar^2}|d_{12}|^2(E_2 - E_1), \quad \text{(C1)}$$

where d_{12} is the dipole matrix element. On the other hand, the spontaneous emission rate, or, equivalently, the transition probability of a generic $|1\rangle \to |2\rangle$ radiative transition, is given by (see, e.g., Ref. 29)

$$\frac{1}{\tau_{\text{spont}}} = W_{1\to 2}^{(2)} S = \frac{\omega_{12}^3 n^3}{3\pi c^3 \hbar \varepsilon}|d_{12}|^2, \quad \text{(C2)}$$

where $W_{1\to 2}^{(2)}$ is the transition probability per unit area, S is the QW area, $\omega_{12} = \frac{E_2 - E_1}{\hbar}$, and ε is the dielectric constant. Substituting $|d_{12}|^2$ from Eq. (C1) into (C2), the oscillator strengths of the $2p \to 1s$ and $|0\rangle \to |2p\rangle$ transitions can be expressed in terms of the transition probability as follows:

$$G^2 \equiv f_{2p\to 1s} = \frac{6\pi c^3 \varepsilon \bar{\mu}_\xi S}{\omega_{\text{THz}}^2 n^3 e^2} W_{2p\to 1s}^{(2)} \quad \text{(C3)}$$

and

$$g^2 \equiv f_{2p} = \frac{6\pi c^3 \varepsilon \bar{\mu}_\xi S}{\omega_{2p}^2 n^3 e^2} W_{2p}^{(2)}, \quad \text{(C4)}$$

where $\omega_{2p} = \frac{E_{2p}}{\hbar}$.

Plugging the above expressions back in Eq. (32), we obtain, for the ratio,

$$r = \frac{\omega_{2p}^2}{\omega_{\text{THz}}^2}\frac{W_{2p\to 1s}^{(2)}}{W_{2p}^{(2)}}. \quad \text{(C5)}$$

*gsk23@bath.ac.uk

[1] M. Tonouchi, Nat. Photonics **1**, 97 (2007).
[2] A. V. Kavokin, I. A. Shelykh, T. Taylor, and M. M. Glazov, Phys. Rev. Lett. **108**, 197401 (2012).
[3] A. D. Jameson, J. J. Tomaino, Y.-S. Lee, J. P. Prineas, J. T. Steiner, M. Kira, and S. W. Koch, Appl. Phys. Lett. **95**, 201107 (2009); J. L. Tomaino, A. D. Jameson, Y.-S. Lee, J. P. Prineas, J. T. Steiner, M. Kira, and S. W. Koch, Solid State Electron. **54**, 1125 (2010).
[4] J. L. Tomaino, A. D. Jameson, Y.-S. Lee, G. Khitrova, H. M. Gibbs, A. C. Klettke, M. Kira, and S. W. Koch, Phys. Rev. Lett. **108**, 267402 (2012).
[5] R. Huber, B. A. Schmid, R. A. Kaindl, and D. S. Chemla, Phys. Status Solidi B **245**, 1041 (2008); R. Huber, R. A. Kaindl, B. A. Schmid, and D. S. Chemla, Phys. Rev. B **72**, 161314(R) (2005).
[6] M. Wagner, H. Schneider, D. Stehr, S. Winnerl, A. M. Andrews, S. Schartner, G. Strasser, and M. Helm, Phys. Rev. Lett. **105**, 167401 (2010).
[7] M. Kira and S. W. Koch, Phys. Rev. Lett. **93**, 076402 (2004).
[8] E. L. Ivchenko, Sov. Phys. Solid State **14**, 2942 (1973).
[9] S. B. Arifzhanov and E. L. Ivchenko, Sov. Phys. Solid State **17**, 46 (1975).
[10] R. D. R. Bhat, P. Nemec, Y. Kerachian, H. M. van Driel, J. E. Sipe, and A. L. Smirl, Phys. Rev. B **71**, 035209 (2005).
[11] G. D. Mahan, Phys. Rev. **170**, 825 (1968).
[12] E. L. Ivchenko and G. E. Pikus, *Superlattices and Other Heterostructures* (Springer, Berlin, 1997).
[13] S. K. Avetissian, A. O. Melikian, and H. R. Minassian, J. Appl. Phys. **80**, 301 (1996).
[14] A. Shimizu, Phys. Rev. B **40**, 1403 (1989).
[15] A. Pasquarello and A. Quattropani, Phys. Rev. B **42**, 9073 (1990).
[16] *Optical Properties of Low-Dimensional Materials*, edited by T. Ogawa and Y. Kanemitsu (World Scientific, Singapore, 1995).
[17] A. A. Pervishko, T. C. H. Liew, V. M. Kovalev, I. G. Savenko, and I. A. Shelykh, Opt. Express **21**, 15183 (2013).
[18] R. J. Elliott, Phys. Rev. **108**, 1384 (1957).
[19] L. C. Hostler, J. Math. Phys. **5**, 591 (1964); Phys. Rev. **178**, 126 (1969).
[20] S. M. Blinder, J. Math. Phys. **25**, 905 (1984).
[21] R. Zimmermann, Phys. Status Solidi B **146**, 371 (1988).
[22] M. Inoue and Y. Toyozawa, J. Phys. Soc. Jpn. **20**, 363 (1965).
[23] V. Heine, *Group Theory in Quantum Mechanics* (Dover, Mineola, NY, 1993).
[24] G. Bastard, *Wave Mechanics Applied to Semiconductor Heterostructures* (Les Editions de Physique, Les Ulis, 1988).
[25] M. Shinada and S. Sugano, J. Phys. Soc. Jpn. **21**, 1936 (1966).
[26] H. Haug and S. W. Koch, *Quantum Theory of the Optical and Electronic Properties of Semiconductors* (World Scientific, Singapore, 1994).
[27] A. I. Anselm, *Introduction to Semiconductor Theory* (MIR, Moscow, 1982).
[28] *Handbook of Mathematical Functions*, edited by M. Abramowitz and I. A. Stegun, Applied Mathematics Series Vol. 55 (National Bureau of Standards, Washington, DC, 1964).
[29] A. Yariv, *Quantum Electronics*, 3rd ed. (Wiley, New York, 1988).